



HHS Public Access

Author manuscript

ACS EST Air. Author manuscript; available in PMC 2025 January 08.

Author Manuscript

Author Manuscript

Author Manuscript

Author Manuscript

Published in final edited form as:

ACS EST Air. 2024 September 16; 1(10): 1317–1328. doi:10.1021/acsestair.4c00150.

Factors Affecting Chlorinated Product Formation from Sodium Hypochlorite Bleach and Limonene Reactions in the Gas Phase

Callee M. Walsh,

Chemical and Biological Monitoring Branch, Health Effects Laboratory Division, National Institute for Occupational Safety and Health, Morgantown, West Virginia 26505, United States

Notashia N. Baughman,

Chemical and Biological Monitoring Branch, Health Effects Laboratory Division, National Institute for Occupational Safety and Health, Morgantown, West Virginia 26505, United States

Jason E. Ham,

Chemical and Biological Monitoring Branch, Health Effects Laboratory Division, National Institute for Occupational Safety and Health, Morgantown, West Virginia 26505, United States

J. R. Wells

Office of the Director, Health Effects Laboratory Division, National Institute for Occupational Safety and Health, Morgantown, West Virginia 26505, United States

Abstract

During use of sodium hypochlorite bleach, gas-phase hypochlorous acid (HOCl) and chlorine (Cl₂) are released, which can react with organic compounds present in indoor air. Reactivity between HOCl/Cl₂ and limonene, a common constituent of indoor air, has been observed.

The purpose of this study was to characterize the chemical species generated from gas-phase reactions between HOCl/Cl₂ and limonene. Gas-phase reactions were prepared in Teflon chambers housing HOCl, Cl₂, and limonene. The resulting chemical products were analyzed using gas-phase preconcentration, followed by gas chromatography and high-resolution mass spectrometry. Several chlorinated products were detected, including limonene species containing one, two, and three chlorines and limonene chlorohydrin. Product concentrations and yields were estimated for the most abundant products, and greater than 80% of transformed limonene was represented in the detected products. Temporal sampling of the reactions allowed time courses to be plotted for limonene decay and chlorinated limonene product generation under different

Corresponding Author Callee M. Walsh – Chemical and Biological Monitoring Branch, Health Effects Laboratory Division, National Institute for Occupational Safety and Health, Morgantown, West Virginia 26505, United States; qqf2@cdc.gov.

ASSOCIATED CONTENT

Supporting Information

The Supporting Information is available free of charge at <https://pubs.acs.org/doi/10.1021/acsestair.4c00150>.

Additional mass spectra and control experiments ([PDF](#))

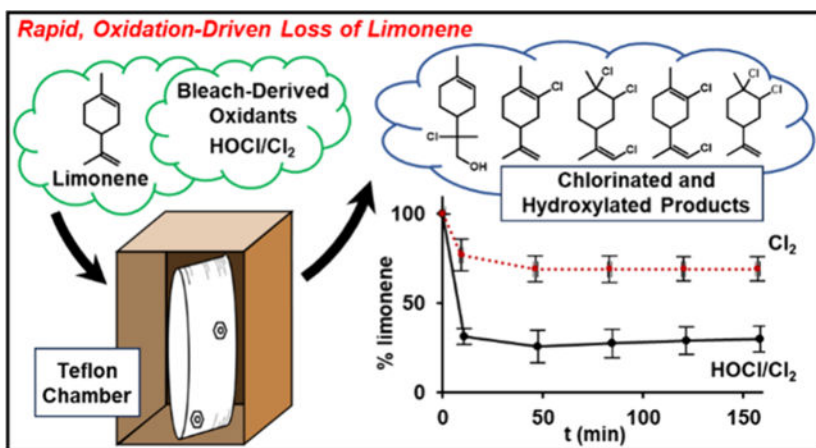
Complete contact information is available at: <https://pubs.acs.org/10.1021/acsestair.4c00150>

The findings and conclusions in this report are those of the authors and do not necessarily represent the official position of the National Institute for Occupational Safety and Health, Centers for Disease Control and Prevention. Mention of any company or product does not constitute endorsement by the National Institute for Occupational Safety and Health, Centers for Disease Control and Prevention.

The authors declare no competing financial interest.

conditions, including the treatments of HOCl/Cl₂, Cl₂ only, high vs low relative humidity, and \pm ozone. These experiments add product speciation, yield estimates, and an understanding of environmental factors affecting product formation to previous studies, further highlighting the chemical transformations initiated by sodium hypochlorite bleach in indoor air.

Graphical Abstract



Keywords

hypochlorous acid; chlorine; indoor; disinfection; chlorohydrin; limonene

INTRODUCTION

Indoor air chemistry is affected by the chemicals introduced into the space, including cleaning products.^{1–4} Concentrations of cleaning product-derived compounds increased indoors during the COVID-19 pandemic due to expanded usage for disinfection.^{5–8} As an example, Zheng et al. reported a 62% increase in cleaning product-derived compounds within household dust during the pandemic compared to prior.⁵ The elevated use of cleaning products within an indoor space can result in unexpected chemistry, leading to potentially hazardous inhalation exposures for occupants.^{9–11} Sodium hypochlorite bleach (i.e., chlorine bleach) is a common disinfectant used in many applications, including water treatment as well as hospital and domestic use in laundry and surface disinfection.¹² Its frequent use is due to the highly effective oxidizing properties of hypochlorous acid (HOCl) on biomolecules.¹³ However, improper mixing of chlorine bleach with acids or ammonia can generate highly toxic chlorine (Cl₂) and chloramine gases (C_xH_xN_xCl_x), respectively.^{13,14} In addition to its acute toxic effects, exposure to chlorine bleach is correlated in several studies with asthma, chronic obstructive pulmonary disease, and respiratory symptoms in occupations where its use is prevalent.^{15–21} These observations warrant additional research to gain a more complete understanding of the impact of chlorine bleach on indoor air chemistry.

Chlorine bleach contributes to the complexity of the indoor air composition. For example, Odabasi and colleagues quantified the presence of chloroform and carbon tetrachloride, both

Author Manuscript

Author Manuscript

Author Manuscript

Author Manuscript

toxic and potentially carcinogenic, in domestic-use bleach.²² The release of chloroform into the gas phase has also been demonstrated during bleach cleaning and laundering activities.^{22,23} Notably, volatilization of the active bleach-derived oxidants, HOCl and Cl₂, has been observed.²⁴ Specifically, during controlled mopping and surface wiping experiments using chlorine bleach products, air concentrations of Cl₂ approaching its 15 min recommended exposure limit (REL) of 500 ppb were measured.²⁵ HOCl concentrations, for which a REL has not been established, were measured in hundreds of ppb.^{24–26}

Additional complexity arises from the propensity of HOCl and Cl₂ to react with common constituents of indoor air and on surfaces, a topic that is rapidly gaining interest in indoor chemistry research.^{27,28} Reactivity occurs with unsaturated organic compounds such as alkenes and dienes. This was demonstrated in heterogeneous reactions between Cl₂ gas and particle phase alkenes in which conversion to dichloroalkanes was observed.^{29–31} While similar products were detected in strictly gas phase experiments, reactivity was less favorable than observed in heterogeneous reactions.^{29,32} For HOCl, electrophilic addition to alkenes was observed in the liquid phase, producing chlorohydrins, which were also detected in heterogeneous reactions between gaseous HOCl and surface films of squalene, oleic acid, and monoterpenes.^{33,34} Recent studies have explored the gas-phase reactivity of HOCl and Cl₂ with the monoterpenes limonene and α -pinene, which are common to indoor air due to cleaning and personal care products.^{35,36} Within environmental chambers and controlled indoor cleaning experiments, mixtures of HOCl/Cl₂ and limonene have yielded chlorinated and oxygenated species.^{37,38} Rapid formation of such species is possible, as the estimated rate constant of HOCl reactivity toward limonene is $2.2 \pm 1.5 \times 10^{-16}$ cm³ molec⁻¹ s⁻¹,³⁷ which is similar to that measured for the reaction of ozone with limonene (2.1×10^{-16} cm³ molec⁻¹ s⁻¹).³⁹ The similar rate constants indicate that HOCl is likely a consequential oxidant in indoor air,⁹ similar to ozone, which has been extensively studied.^{40,41} Additionally, the reactivity of HOCl creates the possibility of competition between multiple oxidants reacting with limonene, which may affect product yields or result in unique product speciation, warranting further evaluation. Collectively, these observations indicate the likelihood for extensive reactivity of HOCl and Cl₂ with organic compounds during routine cleaning activities, the products of which could contribute to exposures for indoor occupants.^{24,37}

Within the current manuscript is a thorough examination of the chemical species generated by reactions between limonene and the gas-phase oxidants, HOCl and Cl₂, released from sodium hypochlorite bleach solutions. Limonene was chosen as a reactant in this study due to its use in prior research, as described above,^{34,37} and its common occurrence in indoor air.⁴² The analysis was carried out using gas chromatography and high-resolution mass spectrometry (GC-HRMS) in order to provide comprehensive product speciation, quantitation of products, and calculation of product yields, information which is limited in existing literature yet important to understand the potential for exposures. In addition, the study was designed to investigate gas-phase reactions of bleach mixtures in the context of common indoor air composition. As such, the effects of typical indoor ozone concentrations and relative humidity were examined. These studies were designed to identify products that could pose exposure risks to occupants and serve as future targets for industrial hygiene monitoring.

METHODS

Chemicals.

Sodium hypochlorite (11–15% active chlorine) and sodium phosphate monobasic monohydrate (99.5%, NaH₂PO₄) were purchased from Thermo Fisher Scientific. Cl₂ compressed gas cylinder (951 ppm of Cl₂, nitrogen balance) and a certified gas standard mixture (17 compounds, ISO 17025 compliant) were purchased from Linde Inc. North America (Alpha, NJ). Limonene (R, +, 99%) was purchased from Sigma-Aldrich (St. Louis, MO). *N,O*-Bis(trimethylsilyl)-trifluoroacetamide (BSTFA, with 1% TMCS) was purchased from Cerilliant Corporation (Round Rock, TX). The endocyclic limonene chlorohydrin products were independently prepared following literature procedures⁴³ to assist in the identification of gas-phase products.

HOCl and Cl₂ Production.

Gaseous HOCl and Cl₂ were produced using procedures adapted from previous studies.^{33,37} To a solution of NaH₂PO₄ (348 mM, pH 4.2) was added NaOCl (11–15% active chlorine) for a final concentration of 367 mM and pH of 6.8; the target pH was chosen to be below the pK_a of HOCl (pH 7.5) in order to maintain HOCl in its undissociated form to facilitate volatilization. Ultrahigh purity nitrogen gas was bubbled at 50 mL/min through this solution. The volatilized HOCl and Cl₂ flowed through Teflon-lined tubing attached to a custom 10 cm UV gas cell (Firefly Sci, Inc., Northport, NY) within a Cary 60 UV/vis spectrophotometer (Agilent, Santa Clara, CA). Following blank correction with nitrogen, the UV absorbances at 242 and 330 nm were monitored for HOCl and Cl₂, respectively. For each experiment, flow was maintained and absorbance data was collected until a steady state concentration was attained, and following this, absorbances were converted to concentrations using Beer's law and corresponding absorption cross sections of $2.03 \times 10^{-19} \text{ cm}^2 \text{ molecule}^{-1}$ for HOCl and $2.55 \times 10^{-19} \text{ cm}^2 \text{ molecule}^{-1}$ for Cl₂.⁴⁴

Chamber Experiments.

Gas-phase reactions were performed in collapsible 100 L Teflon chambers filled with clean air that was prepared by passing compressed house air through anhydrous calcium sulfate (Drierite, Xenia, OH) and 4 Å molecular sieves (Sigma-Aldrich, St. Louis, MO) to eliminate moisture and contaminants. The clean air was then humidified using a bubbler to a desired relative humidity of 5 ± 3% or 50 ± 3%, depending on the experiment. Relative humidity was confirmed with a hygrometer (HMI38, Vaisala, Vantaa, Finland). A separate Teflon chamber containing concentrated, gas-phase limonene (20 ppm) was prepared by passing the cleaned, humidified air through a heated 6.4 mm Swagelok stainless-steel tee into which 10.7 μL limonene (99%) had been injected. The introduction of the conditioned air was controlled by a mass flow controller (GGFC37, Aalborg Instruments and Controls, Inc., Orangeburg, NY) to a flow rate of 5 L/min and a total volume of 80 L. Chambers containing 100 ppb of limonene were created by transferring aliquots from the concentrated 20 ppm limonene chamber to the prepared reaction chamber via 100 mL gastight syringe (Hamilton, Franklin, MA). To prevent photolysis, all experiments were performed in the dark.

HOCl was added to the reaction chamber at the specific mixing ratio of 500 ppb of HOCl to 100 ppb of limonene. Using the concentration of HOCl determined by spectrophotometry (described above), the specific volume of gas needed was determined and was introduced by timed infusion through the bubbler. Cl₂ is inherently produced using this method^{33,37} and, thus, was simultaneously introduced with HOCl during infusion. Cl₂ concentrations averaged 515 ± 45 ppb when the HOCl concentration was held constant at 500 ppb.

Experiments to evaluate the effect of Cl₂ in the absence of HOCl were performed by using a certified standard of compressed Cl₂. The concentration of Cl₂ within the cylinder was 951 ppm ± 2%, and the balance of the cylinder volume was nitrogen. *Caution: Chlorine is classified as a GHS Oxidizing Gas, Category 1; Acute Toxicity (inhalation), Category 2; Skin Corrosion, Category 1; Serious Eye Damage, Category 1; and Aquatic Hazard, Category 1. Working with chlorine gas at high concentrations carries the risk of significant injury or death. For these experiments, chlorine gas was handled within a chemical fume hood while wearing gastight goggles, corrosive-resistant gloves, and half-mask respirators with approved gas/vapor cartridges. Additionally, personal chlorine gas monitors were worn by laboratorians while carrying out these experiments.* Within a chemical fume hood, the Cl₂ was drawn, using airtight tubing from the compressed cylinder, into a small, intermediary Teflon chamber. From there, a gastight syringe was used to transfer the Cl₂ from the intermediate chamber to the 80 L Teflon reaction chambers, producing a final concentration of 500 to 1000 ppb, depending on the experiment.

For experiments incorporating ozone, a mercury pen lamp (Double Bore lamp, Jelight, Irvine, CA) was used to photolyze molecular oxygen. The ozone concentration was measured using a 49i UV photometric ozone monitor (Thermo Fisher, Pittsburgh, PA) and was stored in a small Teflon chamber until use. Immediately at the start of HOCl/Cl₂ infusion, a 100 mL gastight syringe was used to transfer a precise volume of ozone of known concentration to the 80 L limonene reaction chambers, which yielded a final ozone concentration of 30 ppb.

BSTFA Derivatization of Impinger-Collected Gas-Phase Products.

Reactions between limonene (5 ppm) and HOCl/Cl₂ (approximately 5 ppm each) occurred in Teflon chambers (80 L); following this, the reaction products were withdrawn via impingers into 20 mL of acetonitrile at 3 L/min. Higher mixing ratios of reactants were chosen to ensure sufficient hydroxylated product concentrations for derivatization by BSTFA using previously published conditions.⁴⁵ Solvent was evaporated under a stream of dry nitrogen, and the collected products were reconstituted in pyridine and heptane and derivatized using BSTFA at 75 °C for 70 min with agitation. After cooling, samples were analyzed by an Orbitrap GC-MS (Trace 1310 gas chromatograph and Exactive Orbitrap MS, Thermo Scientific) and Agilent GC-MS (7890 GC and 240 EI/CI ion trap MS, Santa Clara, CA).

Gas-Phase Sampling and GC-HRMS.

In order to monitor the gas-phase products from the reaction between limonene and HOCl/Cl₂, immediately after introduction of the bleach oxidants, Teflon chambers were connected

to a 7200 CTS cryogen-free gas preconcentrator (Entech, Simi Valley, CA) coupled to an Orbitrap GC-MS, and 50 mL of the atmosphere within was collected. The first sample was collected at 10 min after the initial infusion of HOCl/Cl₂, and samples were collected at 38 min successively after that as indicated in the figures. From the preconcentrator, the sample was introduced onto the analytical GC column (DB-1, 60 m x 0.25 mm i.d., 1 μ m film thickness, Agilent, Santa Clara, CA) using splitless mode and a sample loading flow program wherein helium began at 0.3 mL/min from 0 to 0.9 min, followed by 1.2 mL/min flow rate through the remainder of the temperature gradient. The temperature gradient consisted of the following: 35 °C held isothermally for 3 min, 10 °C/min ramp rate to a final temperature of 250 °C, followed by an isothermal hold for 0.5 min. The Exactive mass spectrometer data were collected using a scan range of 30 to 500 Da, a resolution of 60,000, and electron ionization (EI) in the positive ion mode. For more definitive molecular ion confirmation, positive chemical ionization (PCI) mode, scanning from 50 to 500 Da, was utilized. The ion source temperature was set to 250 °C for EI and 200 °C for PCI, and the transfer line temperature was 280 and 250 °C for EI and PCI, respectively. Methane was used as the PCI reagent gas at a flow rate of 1.5 mL/min.

Calibration of Chlorinated Limonene Species.

Calibration of gas-phase limonene was performed using an evacuated 6 L Silonite-coated canister that was filled with a known volume of an ISO 17025-compliant, certified VOC standard mixture (Linde Inc., North America) and humidified UHP nitrogen using an Entech 4700 static diluter (Entech, Simi Valley, CA). For calibration, the standardized canister was attached to an Entech 7200 preconcentrator, and varying volumes of gas were sampled to create the concentration range. The total ion current (TIC) peak areas of limonene were integrated (Thermo Xcalibur, version 4.4.16.14) to generate a calibration curve to which TIC peak areas of chlorinated limonene species were calibrated. Yield values were calculated as the concentration of chlorinated product divided by the concentration of the consumed limonene, multiplied by 100.⁴⁶

Data Processing and Analysis.

Mass spectral peak annotation was achieved through high-resolution, accurate mass analysis, which allowed the elemental composition of monoisotopic and fragment ions to be determined. Calculation of elemental composition from *m/z* values was performed in Qual Browser (Thermo Xcalibur, version 4.4.16.14), which were compared to molecular formulas of suspected chlorinated limonene species. Ranges used for elemental composition were as follows: ^{12}C , 0–30; ^{16}O , 0–15; ^1H , 0–60; ^{35}Cl , 0–10; ^{37}Cl , 0–10, and a 5 ppm mass tolerance was used. Mass spectral peak identification was further supported by isotope pattern matching performed in Qual Browser and matching of experimental fragment ions to in silico fragmentation spectra generated in Mass Frontier (Thermo Fisher Scientific, version 8.0.577.177). Chromatographic peak areas for chlorinated limonene species were normalized by the limonene peak area measured at time zero for each experiment. Differences between treatments were determined using Student's *t* test with significance, defined as $p < 0.05$ (JMP software, version 15.1.0, SAS Institute, Cary, NC).

RESULTS AND DISCUSSION

Characterization of Reaction Products.

Gas-phase reactions were initiated between limonene and the volatile constituents of a sodium hypochlorite solution, HOCl and Cl₂, to characterize the species formed. Concentrations of the reactants were selected to mimic realistic concentrations measured in indoor air, specifically 100 ppb limonene and approximately 500 ppb HOCl and 515 ppb Cl₂.^{24–26,47–49} HOCl and Cl₂ were added to limonene in a Teflon chamber housed in the absence of light, and the reaction was monitored temporally using gas-phase sampling followed by GC-MS. The red, dotted trace in Figure 1A, representing the negative control of limonene without added oxidants, indicates that no loss of limonene occurred over the time course. However, 10 min after the introduction of the HOCl/Cl₂ oxidant mixture, a statistically significant 75% reduction in limonene concentration was observed ($p < 0.0001$, Figure 1A, black trace). Later time points (50–160 min) reflected no further decay of limonene.

A representative GC-MS TIC chromatogram collected from the reaction is shown in Figure 1B. With HOCl/Cl₂ addition, shown in the black trace, the limonene peak at RT 18.42 min is reduced to approximately 25%, and several peaks are readily detected at later retention times. The chromatogram from the limonene treatment, shown in red, is largely absent of extraneous peaks beyond limonene.

Table 1 shows the molecular formulas and tentative structures of the limonene reaction products detected in the TIC or extracted ion chromatograms from the limonene + HOCl/Cl₂ treatment. Table S1 contains more detailed information about experimentally measured *m/z* values, fragment ions observed, and their corresponding molecular formulas. Chromatographic peaks at 21.13, 21.59, and 21.80 min were assigned to isomers of singly chlorinated limonene with the molecular ion of *m/z* 170.0857 pertaining to C₁₀H₁₅Cl (Table 1, structure 1, hereafter referred to as **1**). The molecular ion assignment was further confirmed by GC-MS detection using PCI, which resulted in protonation and the expected adduct formation (Figures S1–S3). A fragment at *m/z* 135.1167 resulting from loss of the chlorine atom (C₁₀H₁₅⁺) was observed. Furthermore, the expected isotopic pattern of a 3:1 ratio for C₁₀H₁₅³⁵Cl and C₁₀H₁₅³⁷Cl, respectively, was observed for the parent ion (Figure S4). Current experiments did not allow for definitive assignment of the chlorine position within the structure, but based on previous reports,^{34,50} the chlorine atom is thought to be located on carbons participating in a carbon–carbon double bond. Retention of the double bond in this product could result from a mechanism in which addition of HOCl to the double bond is followed by loss of the hydroxyl group via dehydration prior to mass spectrometric analysis.^{34,50} Structures indicating chlorine addition to both the endocyclic and exocyclic double bonds are shown (Table 1); however, endocyclic addition is likely more favorable, as has been observed for electrophilic addition of ozone to limonene.^{51–54} Although prior evidence suggests that this molecule likely arises from the dehydration of a chlorohydrin species,^{34,50} further work is needed to confirm this assertion.

Peaks at 22.94 and 24.27 min contained *m/z* 206.0624, which corresponds to the molecular ion of C₁₀H₁₆Cl₂, a dichlorinated limonene species (Table 1, structure 2, hereafter referred

Author Manuscript

Author Manuscript

Author Manuscript

Author Manuscript

to as **2**). As expected for molecules containing two chlorine atoms, its molecular ion presented with the characteristic isotopic pattern in the ratio of 9:6:1 for m/z 206.0624 pertaining to $\text{C}_{10}\text{H}_{16}^{35}\text{Cl}_2^+$, m/z 208.0594 pertaining to $\text{C}_{10}\text{H}_{16}^{35}\text{Cl}^{37}\text{Cl}^+$, and m/z 210.0565 corresponding to $\text{C}_{10}\text{H}_{16}^{37}\text{Cl}_2^+$, respectively (Figure S5). A fragment ion at m/z 171.0933 ($\text{C}_{10}\text{H}_{16}\text{Cl}^+$) was present in this spectrum, which was generated through loss of a Cl atom and has been observed previously.³⁷ Loss of both Cl atoms and a hydrogen atom, through intramolecular rearrangement during electron ionization,⁵⁵ resulted in the fragment ion m/z 135.1168 ($\text{C}_{10}\text{H}_{15}^+$), also observed. Generation of the dechlorinated limonene species **2** likely occurs through electrophilic addition of Cl_2 across one of the double bonds.²⁹ This addition could occur at either the endocyclic or exocyclic double bonds, yielding the corresponding isomers designated as **2** in Table 1.

An additional dichlorinated limonene species was detected in peaks at retention times of 24.49, 24.70, 25.10, and 25.15 min. Detected in all peaks was the molecular ion m/z 204.0467 which corresponds to $\text{C}_{10}\text{H}_{14}\text{Cl}_2$ and was further confirmed by PCI and isotopic pattern matching (Figures S6–S9). Chlorine atom position could not be definitively determined experimentally, but chlorine is expected to be bound to one vinylic carbon in each double bond, based on proposed mechanisms in previous reports.³⁴ This species, hereafter termed **3**, is presumed to arise from the addition of HOCl across each double bond, followed by dehydration as discussed above for **1**. A fragment ion m/z 169.0777 ($\text{C}_{10}\text{H}_{14}\text{Cl}^+$) pertaining to loss of a chlorine atom coincided with this parent ion, which has been observed in prior studies.³⁷

Trichlorinated limonene (proposed structure 4, Table 1, hereafter termed **4**) was detected at RT 18.37 and 21.96 min with the molecular ion of m/z 240.0234 corresponding to a molecular formula of $\text{C}_{10}\text{H}_{15}\text{Cl}_3$, using extracted ion chromatogram peak detection. Simultaneously detected in these spectra were m/z 205.0545 pertaining to the loss of a chlorine atom ($\text{C}_{10}\text{H}_{15}\text{Cl}_2^+$) and m/z 169.0778 corresponding to the loss of two chlorine atoms and one hydrogen ($\text{C}_{10}\text{H}_{14}\text{Cl}^+$). Further, the observed isotopic pattern matched that expected theoretically for the two most abundant isotopes; the additional isotopes were not detected, likely due to a low concentration (see Figure S10).

Finally, limonene chlorohydrins were identified at RT 23.56 and 23.63 min, which have the molecular ion m/z 188.0962 and molecular formula $\text{C}_{10}\text{H}_{17}\text{ClO}$ (structure 5, Table 1, hereafter referred to as **5**). The presence of the hydroxyl group was confirmed by its reaction with BSTFA, resulting in the corresponding trimethylsilyl derivative (Figure S11). For the underivatized molecule, the fragment ion m/z 173.0725 ($\text{C}_9\text{H}_{14}\text{ClO}^+$) was detected which corresponded to a loss of a methyl group, and fragment ion at m/z 153.1271 pertained to loss of the chlorine atom ($\text{C}_{10}\text{H}_{17}\text{O}^+$). Comparison of fragmentation patterns to previously published work⁵⁶ indicate that the chlorohydrin functional group of these molecules resides on the carbons previously participating in the exocyclic carbon–carbon double bond. The position of the chlorohydrin functional group was further confirmed through a comparison of gas-phase products to a synthesized endocyclic chlorohydrin standard. Comparison of the GC-MS chromatograms between the samples indicates, as shown in Figure S12, that for reactions in the gas phase, endocyclic chlorohydrin is not formed at appreciable levels. This contrasts with solution phase chlorination of limonene, where both endocyclic

Author Manuscript

Author Manuscript

Author Manuscript

Author Manuscript

and exocyclic chlorohydrin formation were observed.⁵⁶ Given previous evidence for the electrophilic addition of ozone preferentially to the endocyclic double bond of limonene, the corresponding endocyclic limonene chlorohydrin was assumed to be the more favorable species; therefore, its negligible formation is unexpected. This observation may indicate rapid conversion of endocyclic limonene chlorohydrin to other species, presumably **1** and **3**, via dehydration within 10 min. Supporting the possibility of rapid dehydration, acid-catalyzed dehydration of hydroxycarbonyls to dihydrofurans in the heterogeneous phase have been observed in similar time scales.⁵⁷

Additional limonene species that contained oxygenated functional groups were expected based on recent work.³⁴ In the current study, *m/z* 186.0806 pertaining to chlorinated limonene with a hydroxyl group addition was detected with a molecular formula of C₁₀H₁₅OCl (Figure S13) at RT 22.31 min, and the presence of the hydroxyl group was confirmed with BSTFA derivatization (Figure S14); however, abundance appears to be low.

Chlorinated Limonene Product Yield Estimates.

To provide additional insight into the potential for exposure, the yields of the oxygenated and chlorinated species generated in the gas-phase reactions were measured. Many of the species were not commercially available; as such, a surrogate approach was employed (see methods section). This approach and its corresponding calibration curve (Figure S15) were applied to the largest peaks discernible from the TIC chromatogram at the first time point (10 min) of temporal sampling experiments. Yield values were calculated as the concentration of chlorinated product divided by the concentration of the consumed limonene.⁴⁶ At the lower end of the calibration curve, higher variability was observed, which affected the quantitation accuracy; thus, many of the smaller peaks, such as those pertaining to **2**, were excluded from the estimates. As shown in Table S1, for the singly chlorinated product **1**, at RT 21.6 min, the estimated yield was 57 ± 8.7%, which was the highest yield of all species. The peaks pertaining to **3** at RT 24.70, 25.10, and 25.15 min followed with a total of 28% yield. It should be noted that the yield listed for the peak at 25.15 min was the combined area across both 25.10 and 25.15 min, as these peaks were unresolvable chromatographically.

The yield data provide insight into the mechanisms of product formation among limonene, HOCl, and Cl₂. The estimated HOCl gas-phase rate constant for limonene exceeds that of Cl₂ by an order of magnitude (2.2 ± 1.5 × 10⁻¹⁶ vs 1.6 × 10⁻¹⁷ cm³ molec⁻¹ s⁻¹, respectively).³⁷ It follows that **1** and **3**, which are thought to arise from HOCl, are found in higher yield versus **2**, of which Cl₂ is the progenitor. The low abundance (estimated at <1 ppb) of the chlorohydrin products was unexpected when compared to previous studies in which these species were detected readily.^{33,34} The formation of particulate matter during the gas-phase reactions could affect the detectability of chlorohydrin species. Supporting this hypothesis, the estimated vapor pressure, calculated using EPI Suite,⁵⁸ for the limonene chlorohydrin species (0.001 mmHg) was substantially lower than limonene (1.98 mmHg), **1** (0.7 mmHg), and **2** (0.1 mmHg). However, experimental evidence did not confirm the formation of particulate matter. Specifically, SMPS measurements recorded for over 60 min indicate particles were not detected in reactions between limonene and HOCl/Cl₂ in

the absence of light (data not shown), which matches results of others.³⁷ Additionally, in prepared chambers of the synthesized limonene chlorohydrin, its stability in the gas phase was observed for several hours, indicating the lack of loss to particles or chamber walls due to low volatility (Figure S16). Other factors affecting the detection of chlorohydrin species between the current study and others could include variations in parameters such as the relative humidity or the ratios of HOCl to Cl₂. Alternatively, it is possible that the limonene chlorohydrin species were not detected due to rapid dehydration to other products, such as **1** and **3** as discussed above. Future studies could include an online sampling method to permit more rapid detection of these presumably transient chlorohydrin species as well as the incorporation of a derivatization strategy to detect these oxygenated species more readily via GC-MS. Despite this, the above estimates indicate that 85% of the loss of limonene is accounted for in species **1** and **3** within 10 min of reaction, and the concentrations of some individual species were detected within the range of 20 to 50 ppb.

Comparison between the Effect of Cl₂ and HOCl/Cl₂ on Limonene Product Speciation.

To better elucidate the mechanisms of product formation, the independent contributions of HOCl and Cl₂ were investigated. Because HOCl is in equilibrium with Cl₂ and, therefore, cannot be isolated, pure Cl₂ was compared to the mixture of HOCl/Cl₂ derived from sodium hypochlorite. Several replicate experiments were performed in which 500 and 1000 ppb chlorine was added to the limonene chambers, and temporal sampling was performed. The 1000 ppb chlorine treatment was initially chosen to more closely match the total number of chlorine-containing oxidant molecules present in the HOCl/Cl₂ treatment, which contained approximately 500 ppb HOCl/515 ppb Cl₂. However, as minimal differences between the two concentrations of Cl₂ were observed (Figure S17), the data for both 500 and 1000 ppb chlorine were averaged and are presented in Figure 2 (red, dotted trace). Exposure of limonene to 500–1000 ppb Cl₂ across several experiments caused only a 22% reduction in limonene which was significantly different from the 70% reduction observed for the mixture of HOCl/Cl₂ at 10 min ($p < 0.0001$, Figure 2, panel A), supporting the larger role of HOCl in the reaction mechanism.

Formation patterns of representative chlorinated products were tracked simultaneously with the decay of limonene for 160 min. For the limonene + HOCl/Cl₂ reactions (black trace), differences were observed in the temporal patterns of product formation across the three representative chlorinated limonene species. Specifically, product formation reached a plateau at the second time point of 50 min for **1** (panel B) and **2** (panel C). The chlorohydrin product (**5**, Figure 2, panel D) formed two times more slowly, as the maximum amount of product stabilized by the fourth time point, approximately 120 min after reaction initiation. This result may indicate that most of the chlorohydrin species formed are converted rapidly and undetectably using current measurements to a singly chlorinated species through dehydration as discussed previously.

For the Cl₂ treatment, as shown in Figure 2 (red, dotted traces), all of the same products were generated, but the concentrations were significantly reduced relative to the HOCl/Cl₂ treatment (all $p < 0.02$ at 10 min). At the 10 min time point, 49% less compound **2** was detected in the Cl₂ treatment compared to HOCl/Cl₂ treatment (panel C, $p = 0.014$).

However, such an effect on this product was not expected because concentrations of Cl_2 were similar between Cl_2 and HOCl/Cl_2 treatments, and Cl_2 is thought to be its main progenitor. These results may indicate the involvement of HOCl or other incidental compounds, facilitating its formation. In support, recent studies indicate that heterogeneous reaction kinetics of Cl_2 are enhanced in the presence of oxygenated molecules.³¹ The Cl_2 data for **1**, **3**, and **5** support the idea that HOCl has a greater role in their formation (Figures 2 and S18). Formation of the singly chlorinated limonene (**1**, panel B) and limonene chlorohydrin (**5**, panel D) were attenuated to a larger degree in the Cl_2 treatment, 68% and 91%, respectively, than that of **2** (49% reduction, panel C). Similarly, the peaks pertaining to **3**, which is also thought to originate from HOCl , were more severely attenuated in the Cl_2 treatment (79–84%; see Figure S18) compared to the attenuation of **2**. It was unanticipated that **1**, **3**, and **5** were formed at appreciable levels in the Cl_2 treatment, because these molecules are presumed to arise strictly from HOCl . This suggests that an alternative pathway for the formation of these chlorinated species could be involved. For the formation of these species to occur in the Cl_2 treatment, the presence of water vapor within the chamber may be necessary (50% RH in these experiments), as Cl_2 is known to react with water to form HOCl . Additional experimentation was conducted to determine the effect of relative humidity on product formation (see below).

Effect of Relative Humidity on Limonene Product Speciation and Amounts.

The effect of relative humidity (RH) on product formation was investigated through limonene reactions prepared with HOCl/Cl_2 and Cl_2 alone at 50% (high) and 5% RH (low). Control experiments containing limonene without added oxidants indicate its stability at both low (Figure S19) and high RH in Teflon chambers (see Figure 1A, red dotted trace). For the Cl_2 reactions, limonene decay was unexpectedly enhanced in low humidity conditions (58% loss in low humidity vs 22% loss in high humidity conditions; Figure 3, panel A; $p = 0.0019$, 10 min time point). However, a concomitant increase in the concentration of chlorinated limonene products was not observed. Specifically, as shown in Figure 3, low humidity had no significant effect on the formation of **1** (panel B; $p = 0.89$, 10 min) and **2** (panel C; $p = 0.54$, 10 min), indicating that the RH percentages chosen for this experiment do not significantly affect product formation in the Cl_2 treatment. Conversely, a significant reduction in limonene chlorohydrin product (**5**, panel D; $p = 0.026$, at 80 min) was observed in low humidity conditions, which indicates a more sensitive dependence on %RH for its formation when only Cl_2 is present. In fact, in the low RH treatment, chlorohydrin formation was undetectable. The enhanced decay of limonene in the low humidity conditions cannot be explained by changes in the targeted products, and therefore, these data may suggest that additional products were generated in the low humidity conditions, which are unaccounted for in the employed sampling strategy.

The effect of humidity on product formation using the bleach oxidant mixture was investigated, as well. Similarly, to that observed for limonene/ Cl_2 reactions in low humidity, the introduction of HOCl/Cl_2 to limonene in low humidity conditions caused an increase in limonene decay compared to 50% RH conditions (98% loss at low RH vs 70% loss at high RH; $p = 0.0015$, 10 min time point). This observation may indicate that in low RH conditions more HOCl/Cl_2 is available as a result of less reaction with water

vapor. However, a corresponding increase in the chlorinated product formation was not observed. As shown in Figure 4, significantly less formation occurred for all products in low humidity conditions in the limonene + HOCl/Cl₂ treatments (all $p < 0.02$ at 10 min). The singly chlorinated (**1**, panel B) and dichlorinated products (**2**, panel C) were attenuated by approximately 60%, and the chlorohydrin (**5**, panel D) was attenuated by greater than 90% at 10 min. In contrast to the results in Figure 3, where humidity had no effect on the singly and doubly chlorinated limonene product formation with Cl₂ only, these results demonstrate a significant role of RH in the enhancement of the HOCl-initiated product formation for **1**, **2**, and **5**. Again, as above, the additional limonene loss observed in low humidity conditions could not be accounted for by the selected products, and the loss may be due to alternative products that went undetected with current sampling strategies. Overall, these results demonstrate a significant role of water vapor in facilitating chlorinated and chlorohydrin product formation and may have implications for real world exposures in humid environments where bleach application is performed.

Effect of Ozone on Limonene Product Speciation and Amounts.

To better represent the conditions in indoor air, the effect of ozone was explored in the context of the HOCl/Cl₂ reactions with limonene. Ozone reacts readily with terpenes at sites of unsaturation, resulting in carbonyl-containing products which remain in the gas phase.¹ Furthermore, the formation of Criegee intermediates during ozonolysis causes hydroxyl radical formation and semivolatile product formation, such as peroxides and organic acids, resulting in the formation of secondary organic aerosol.¹ Experiments were performed to determine how the competition between multiple oxidants affected the rate of the reaction, as well as product formation. Ozone was added simultaneously along with the HOCl/Cl₂ mixture to chambers containing 100 ppb limonene. The final concentrations were 30 ppb ozone, which is an indoor air concentration possible with high air exchange rates,^{41,59} and 500 ppb HOCl/515 ppb Cl₂. As shown in Figure 5, the addition of ozone did not influence the decay of limonene at the initial time points of 10 and 50 min, but as the reaction proceeded, a statistically significant ($p = 0.04$) enhancement of limonene loss was observed by approximately 80 min, which was sustained through 160 min (panel A). Ozone caused a 37% reduction in limonene chlorohydrin formation at 50 min (**5**, panel D), though high error in the HOCl/Cl₂ treatment precluded the comparison from reaching statistical significance ($p = 0.49$). A statistically significant 25% and 36% reduction in the formation of the singly chlorinated (**1**, panel B; $p = 0.02$) and dichlorinated limonene product (**2**, panel C; $p = 0.046$), respectively, was observed at the 50 min time point and beyond in the presence of O₃. These results are consistent with the experimental rate constants reported for each oxidant of 1.6×10^{-17} , $2.2 (\pm 1.5) \times 10^{-16}$, and $2.1 \times 10^{-16} \text{ cm}^3 \text{ molecule}^{-1} \text{ s}^{-1}$ for Cl₂, HOCl, and O₃.^{37,60} For these chlorinated products, the data indicate that even at the low concentration used in the experiments, ozone could effectively compete with Cl₂ and HOCl, which were present at greater than 10-fold its excess. The results suggest that the low concentration of ozone can meaningfully attenuate HOCl/Cl₂-initiated product formation at ratios used in the current experiments.

Significance and Implications.

We describe the formation of chlorinated and oxygenated products generated from the gas-phase reaction between limonene and HOCl/Cl₂ and characterize the species by GC-HRMS. Data herein provide evidence for the formation of additional species including singly chlorinated (**1**), dichlorinated (**2**), and trichlorinated (**4**) limonene compared to those recently described on surfaces and in the gas phase.³⁴ Experimental evidence was presented describing additional indoor environmental factors that affect product formation, including relative humidity and ozone competition. Specifically, higher relative humidity significantly enhances product formation for chlorinated limonene species; conversely, typical indoor concentrations of ozone suppressed the product yield. In addition, data indicate that chlorinated limonene species are produced rapidly upon reaction initiation and remain stable for more than 2 h. Specifically, from this study using realistic indoor air concentrations, some species reached near peak formation and limonene reached peak decay at 10 min. Using these data, a minimum limonene loss rate of 6 h⁻¹ can be estimated, which indicates the loss of limonene via the HOCl/Cl₂ reaction is 12 times greater than the typical air exchange rate of 0.5 h⁻¹. This rate is comparable to that calculated using the published HOCl/limonene rate constant ($k_{\text{HOCl}/\text{limonene}} = 2.2 \pm 1.5 \times 10^{-16} \text{ cm}^3 \text{ molec}^{-1} \text{ s}^{-1}$)³⁷ and an initial HOCl concentration of 500 ppb, which resulted in the limonene loss rate constant ($K' = [\text{HOCl}](k_{\text{HOCl}/\text{limonene}})$) being 20 times faster than air exchange. Collectively, these data indicate that such reactions have the potential to form products in time scales capable of causing exposures to indoor occupants.

The sampling strategy used in this study enabled concentrations and yields of some chlorinated species to be estimated, which have not been previously reported in similar studies of sodium hypochlorite bleach. The yield for the most abundant species, the singly chlorinated limonene compound **1**, was estimated to total 57% of the consumed limonene, which would equate to approximately 46 ppb using the reactant concentrations in these experiments. Although exposure limits are not available for chlorinated limonene compounds, this concentration falls below 15 min recommended exposure limits for other volatile chlorinated compounds such as chloroform, chloromethylbenzene, and chlorobutadiene which are 2, 1, and 1 ppm, respectively.⁶¹ Though it is not likely that chlorinated limonene species cause acute toxicity at concentrations observed in this study, the effects of long-term exposure should be examined further. For example, the connection between exposure to mixtures of chemicals at low concentrations and the development of cancer is a growing area of research.^{62,63} Furthermore, it is likely that chlorine-generated species could reach higher levels than were observed in this study given the concentrations of limonene and HOCl that have been measured, previously.^{24,26,49} Overall, this work further characterizes the products formed, enhances our understanding of how multiple oxidants impact a reaction system, and increases our understanding of conditions affecting chlorinated product formation. Cumulatively, these data and those of others highlight the importance of additional research to understand the impact of sodium hypochlorite bleach on indoor air composition.

Supplementary Material

Refer to Web version on PubMed Central for supplementary material.

Funding

This work was supported by intramural funds (CAN #9390KJZ) from the National Institute for Occupational Safety and Health, Centers for Disease Control and Prevention.

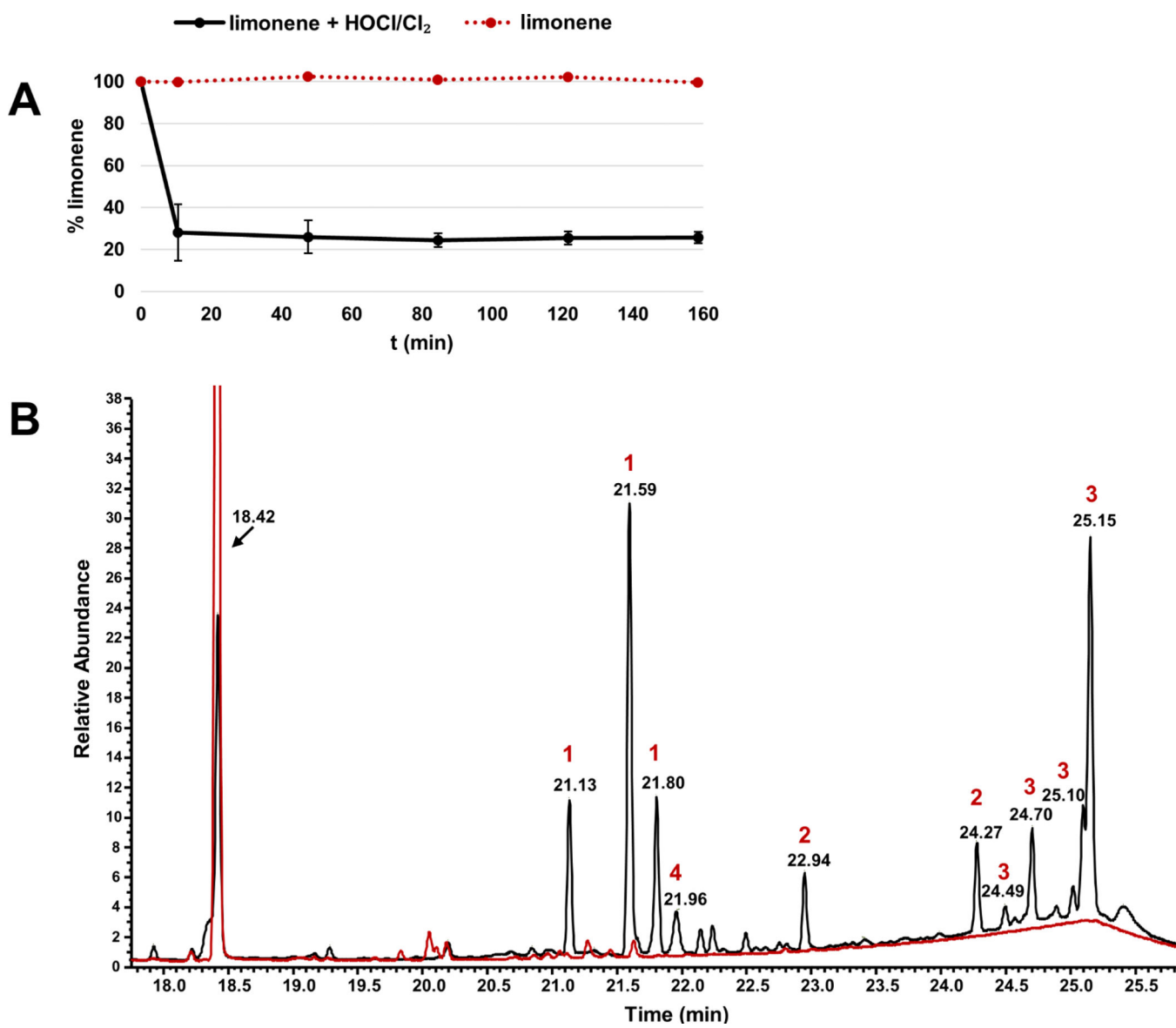
REFERENCES

- (1). Nazaroff WW; Weschler CJ Cleaning products and air fresheners: exposure to primary and secondary air pollutants. *Atmos. Environ.* 2004, 38 (18), 2841–2865.
- (2). Weschler CJ; Carslaw N. Indoor Chemistry. *Environ. Sci. Technol.* 2018, 52 (5), 2419–2428. [PubMed: 29402076]
- (3). Gligorovski S; Abbatt JPD An indoor chemical cocktail. *Science* 2018, 359 (6376), 632–633. [PubMed: 29439226]
- (4). Ault AP; Grassian VH; Carslaw N; Collins DB; Destaillats H; Donaldson DJ; Farmer DK; Jimenez JL; McNeill VF; Morrison GC; et al. Indoor surface chemistry: developing a molecular picture of reactions on indoor interfaces. *Chem* 2020, 6 (12), 3203–3218. [PubMed: 32984643]
- (5). Zheng G; Filippelli GM; Salamova A. Increased Indoor Exposure to Commonly Used Disinfectants during the COVID-19 Pandemic. *Environmental Science & Technology Letters* 2020, 7 (10), 760–765. [PubMed: 37566290]
- (6). Chang A; Schnall AH; Law R; Bronstein AC; Marraffa JM; Spiller HA; Hays HL; Funk AR; Mercurio-Zappala M; Calello DP; et al. Cleaning and disinfectant chemical exposures and temporal associations with COVID-19 - National poison data system, United States, January 1, 2020–March 31, 2020. *Morbidity and Mortality Weekly Report* 2020, 69 (16), 496–498. [PubMed: 32324720]
- (7). Dewey HM; Jones JM; Keating MR; Budhathoki-Uprety J. Increased use of disinfectants during the COVID-19 pandemic and its potential impacts on health and safety. *ACS Chemical Health & Safety* 2022, 29 (1), 27–38.
- (8). How COVID-19 has transformed consumer spending, 2020. <https://www.jpmorgan.com/insights/global-research/retail/covid-spending-habits> (accessed 2024 August 2).
- (9). Collins DB; Farmer DK Unintended Consequences of Air Cleaning Chemistry. *Environ. Sci. Technol.* 2021, 55 (18), 12172–12179. [PubMed: 34464124]
- (10). Carslaw N; Fletcher L; Heard D; Ingham T; Walker H. Significant OH production under surface cleaning and air cleaning conditions: Impact on indoor air quality. *Indoor Air* 2017, 27 (6), 1091–1100. [PubMed: 28493625]
- (11). Wang Z; Kowal SF; Carslaw N; Kahan TF Photolysis-driven indoor air chemistry following cleaning of hospital wards. *Indoor Air* 2020, 30 (6), 1241–1255. [PubMed: 32485006]
- (12). Coons DM Bleach: Facts, fantasy, and fundamentals. *J. Am. Oil Chem. Soc* 1978, 55 (1), 104–108.
- (13). Rutala WA; Weber DJ Uses of inorganic hypochlorite (bleach) in health-care facilities. *Clin. Microbiol. Rev* 1997, 10 (4), 597–610. [PubMed: 9336664]
- (14). Boerner LK Accidental mix of bleach and acid kills Buffalo Wild Wings employee. *Chemical and Engineering News; American Chemical Society*, 2019; Vol. 97.
- (15). Clausen PA; Frederiksen M; Sejbæk CS; Sorli JB; Hougaard KS; Frydendall KB; Caroe TK; Flachs EM; Meyer HW; Schlünssen, V.; Wolkoff, P. Chemicals inhaled from spray cleaning and disinfection products and their respiratory effects. A comprehensive review. *International Journal of Hygiene and Environmental Health* 2020, 229, No. 113592.
- (16). Dumas O; Wiley AS; Quinot C; Varraso R; Zock JP; Henneberger PK; Speizer FE; Le Moual N; Camargo CA Jr. Occupational exposure to disinfectants and asthma control in US nurses. *Eur. Respir. J* 2017, 50 (4), 1700237.

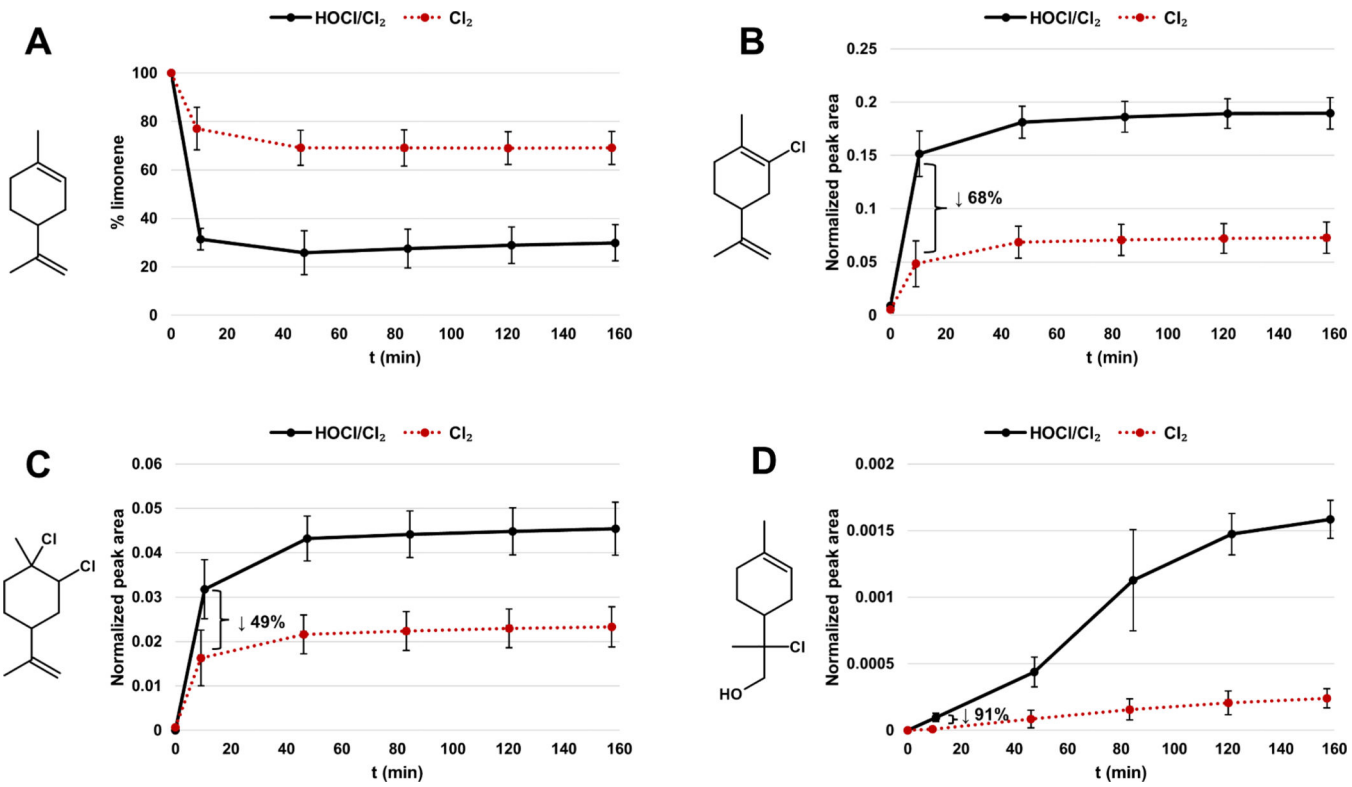
- (17). Dumas O; Varraso R; Boggs KM; Quinot C; Zock J-P; Henneberger PK; Speizer FE; Le Moual N; Camargo CA Jr. Association of Occupational Exposure to Disinfectants With Incidence of Chronic Obstructive Pulmonary Disease Among US Female Nurses. *JAMA Network Open* 2019, 2 (10), e1913563–e1913563.
- (18). Zock JP; Vizcaya D; Le Moual N. Update on asthma and cleaners. *Curr. Opin Allergy Clin Immunol* 2010, 10 (2), 114–120. [PubMed: 20093933]
- (19). Mirabelli MC; Zock J-P; Plana E; Antó JM; Benke G; Blanc PD; Dahlman-Höglund A; Jarvis DL; Kromhout H; Lillienberg L; et al. Occupational risk factors for asthma among nurses and related health care professionals in an international study. *Occupational and Environmental Medicine* 2007, 64, 474–479. [PubMed: 17332135]
- (20). Quinn MM; Henneberger PK; Braun B; Delclos GL; Fagan K; Huang V; Knaack JL; Kusek L; Lee S-J; Le Moual N; et al. Cleaning and disinfecting environmental surfaces in health care: toward an integrated framework for infection and occupational illness prevention. *American Journal of Infection Control* 2015, 43 (5), 424–434. [PubMed: 25792102]
- (21). Patel J; Gimeno Ruiz de Porras D; Mitchell LE; Carson A; Whitehead LW; Han I; Pompeii L; Conway S; Zock J-P; Henneberger PK; Patel R; Reyes JDL; Delclos GL. Cleaning Tasks and Products and Asthma Among Health Care Professionals. *J. Occup Environ. Med* 2024, 66 (1), 28–34. [PubMed: 37801602]
- (22). Odabasi M. Halogenated volatile organic compounds from the use of chlorine-bleach-containing household products. *Environ. Sci. Technol* 2008, 42 (5), 1445–1451. [PubMed: 18441786]
- (23). Shepherd JL; Corsi RL; Kemp J. Chloroform in Indoor Air and Wastewater: The Role of Residential Washing Machines. *J. Air Waste Manage. Assoc* 1996, 46 (7), 631–642.
- (24). Wong JPS; Carslaw N; Zhao R; Zhou S; Abbatt JPD. Observations and impacts of bleach washing on indoor chlorine chemistry. *Indoor Air* 2017, 27 (6), 1082–1090. [PubMed: 28646605]
- (25). Mattila JM; Lakey PSJ; Shiraiwa M; Wang C; Abbatt JPD; Arata C; Goldstein AH; Ampollini L; Katz EF; DeCarlo PF; et al. Multiphase Chemistry Controls Inorganic Chlorinated and Nitrogenated Compounds in Indoor Air during Bleach Cleaning. *Environ. Sci. Technol* 2020, 54 (3), 1730–1739. [PubMed: 31940195]
- (26). Stubbs AD; Lao M; Wang C; Abbatt JP; Hoffnagle J; VandenBoer TC; Kahan TF. Near-source hypochlorous acid emissions from indoor bleach cleaning. *Environmental Science: Processes & Impacts* 2023, 25 (1), 56–65. [PubMed: 36602445]
- (27). Jahn LG; Bhattacharyya N; Blomdahl D; Tang M; Abue P; Novoselac A; Ruiz LH; Misztal PK. Influence of Application Method on Disinfectant Byproduct Formation during Indoor Bleach Cleaning: A Case Study on Phenol Chlorination. *ACS ES&T Air* 2024, 1 (1), 16–24.
- (28). Wang C; Mattila JM; Farmer DK; Arata C; Goldstein AH; Abbatt JP. Behavior of isocyanic acid and other nitrogen-containing volatile organic compounds in the indoor environment. *Environ. Sci. Technol* 2022, 56 (12), 7598–7607. [PubMed: 35653434]
- (29). Popolan-Vaida DM; Liu C-L; Nah T; Wilson KR; Leone SR. Reaction of Chlorine Molecules with Unsaturated Submicron Organic Particles. *Zeitschrift für Physikalische Chemie* 2015, 229 (10–12), 1521–1540.
- (30). Zeng M; Liu C-L; Wilson KR. Catalytic Coupling of Free Radical Oxidation and Electrophilic Chlorine Addition by Phase-Transfer Intermediates in Liquid Aerosols. *J. Phys. Chem. A* 2022, 126 (19), 2959–2965. [PubMed: 35511037]
- (31). Zeng M; Wilson KR. Experimental evidence that halogen bonding catalyzes the heterogeneous chlorination of alkenes in submicron liquid droplets. *Chemical science* 2021, 12 (31), 10455–10466. [PubMed: 34447538]
- (32). Groll H; Hearne G; Rust F; Vaughan W. HALOGENATION OF HYDROCARBONS. Chlorination of Olefins and Olefin-Paraffin Mixtures at Moderate Temperatures. Induced Substitution. *Industrial & Engineering Chemistry* 1939, 31 (10), 1239–1244.
- (33). Schwartz-Narbonne H; Wang C; Zhou S; Abbatt JPD; Faust J. Heterogeneous Chlorination of Squalene and Oleic Acid. *Environ. Sci. Technol* 2019, 53 (3), 1217–1224, Article. DOI: [PubMed: 30387352]
- (34). Deleepojananan C; Grassian VH. Gas-Phase and Surface-Initiated Reactions of Household Bleach and Terpene-Containing Cleaning Products Yield Chlorination and Oxidation Products

- Adsorbed onto Indoor Relevant Surfaces. *Environ. Sci. Technol.* 2023, 57 (49), 20699–20707. [PubMed: 38010858]
- (35). Sarwar G; Olson DA; Corsi RL; Weschler CJ Indoor Fine Particles: The Role of Terpene Emissions from Consumer Products. *J. Air Waste Manage. Assoc.* 2004, 54 (3), 367–377.
- (36). Steinemann AC Fragranced consumer products and undisclosed ingredients. *Environmental Impact Assessment Review* 2009, 29 (1), 32–38.
- (37). Wang C; Collins DB; Abbatt JPD Indoor Illumination of Terpenes and Bleach Emissions Leads to Particle Formation and Growth. *Environ. Sci. Technol.* 2019, 53 (20), 11792–11800. [PubMed: 31576741]
- (38). Mattila JM; Arata C; Wang C; Katz EF; Abeleira A; Zhou Y; Zhou S; Goldstein AH; Abbatt JPD; DeCarlo PF; Farmer DK Dark Chemistry during Bleach Cleaning Enhances Oxidation of Organics and Secondary Organic Aerosol Production Indoors. *Environmental Science & Technology Letters* 2020, 7 (11), 795–801.
- (39). Atkinson R; Arey J. Atmospheric degradation of volatile organic compounds. *Chem. Rev.* 2003, 103 (12), 4605–4638. [PubMed: 14664626]
- (40). Coffaro B; Weisel CP Reactions and Products of Squalene and Ozone: A Review. *Environ. Sci. Technol.* 2022, 56 (12), 7396–7411. [PubMed: 35648815]
- (41). Weschler CJ Ozone in indoor environments: concentration and chemistry. *Indoor Air* 2000, 10, 269–288. [PubMed: 11089331]
- (42). Wainman T; Zhang J; Weschler CJ; Liou PJ Ozone and limonene in indoor air: a source of submicron particle exposure. *Environ. Health Perspect.* 2000, 108 (12), 1139–1145. [PubMed: 11133393]
- (43). Nishitani K; Shinya K; Yamakawa K. An alternative regioselective ring-opening of epoxides to chlorohydrins mediated by chlorotitanium (IV) reagents. *Heterocycles* 2007, 74, 191–197.
- (44). Burkholder JB; Sander SP; Abbatt JPD; Barker JR; Huie RE; Kolb CE; Kurylo MJ; Orkin VL; Wilmouth DM; Wine PH Chemical Kinetics and Photochemical Data for Use in Atmospheric Studies, Evaluation No. 18. JPL Publication 15–10, 2015. https://jpldataeval.jpl.nasa.gov/pdf/JPL_Publication_15-10.pdf.
- (45). Pietrogrande MC; Bacco D. GC–MS analysis of water-soluble organics in atmospheric aerosol: Response surface method-ology for optimizing silyl-derivatization for simultaneous analysis of carboxylic acids and sugars. *Anal. Chim. Acta* 2011, 689 (2), 257–264. [PubMed: 21397082]
- (46). Gao S; Keywood M; Ng NL; Surratt J; Varutbangkul V; Bahreini R; Flagan RC; Seinfeld JH Low-molecular-weight and oligomeric components in secondary organic aerosol from the ozonolysis of cycloalkenes and α -pinene. *J. Phys. Chem. A* 2004, 108 (46), 10147–10164.
- (47). Riveron TP; Wilde MJ; Ibrahim W; Carr L; Monks PS; Greening NJ; Gaillard EA; Brightling CE; Siddiqui S; Hansell AL; Cordell RL Characterisation of volatile organic compounds in hospital indoor air and exposure health risk determination. *Building and Environment* 2023, 242, No. 110513.
- (48). Geiss O; Giannopoulos G; Tirendi S; Barrero-Moreno J; Larsen BR; Kotzias D. The AIRMEX study - VOC measurements in public buildings and schools/kindergartens in eleven European cities: Statistical analysis of the data. *Atmos. Environ.* 2011, 45 (22), 3676–3684.
- (49). Singer BC; Coleman BK; Destaillats H; Hodgson AT; Lunden MM; Weschler CJ; Nazaroff WW Indoor secondary pollutants from cleaning product and air freshener use in the presence of ozone. *Atmos. Environ.* 2006, 40 (35), 6696–6710.
- (50). Jorga SD; Liu T; Wang Y; Hassan S; Huynh H; Abbatt JPD Kinetics of hypochlorous acid reactions with organic and chloride-containing tropospheric aerosol. *Environmental Science: Processes & Impacts* 2023, 25 (10), 1645–1656. [PubMed: 37721367]
- (51). Calogirou A; Larsen BR; Kotzias D. Gas-phase terpene oxidation products: a review. *Atmos. Environ.* 1999, 33 (9), 1423–1439.
- (52). Zhang J; Huff Hartz KE; Pandis SN; Donahue NM Secondary Organic Aerosol Formation from Limonene Ozonolysis: Homogeneous and Heterogeneous Influences as a Function of NO_x. *J. Phys. Chem. A* 2006, 110 (38), 11053–11063. [PubMed: 16986838]
- (53). Jiang L; Wang W; Xu Y. Ab initio investigation of O₃ addition to double bonds of limonene. *Chem. Phys.* 2010, 368 (3), 108–112.

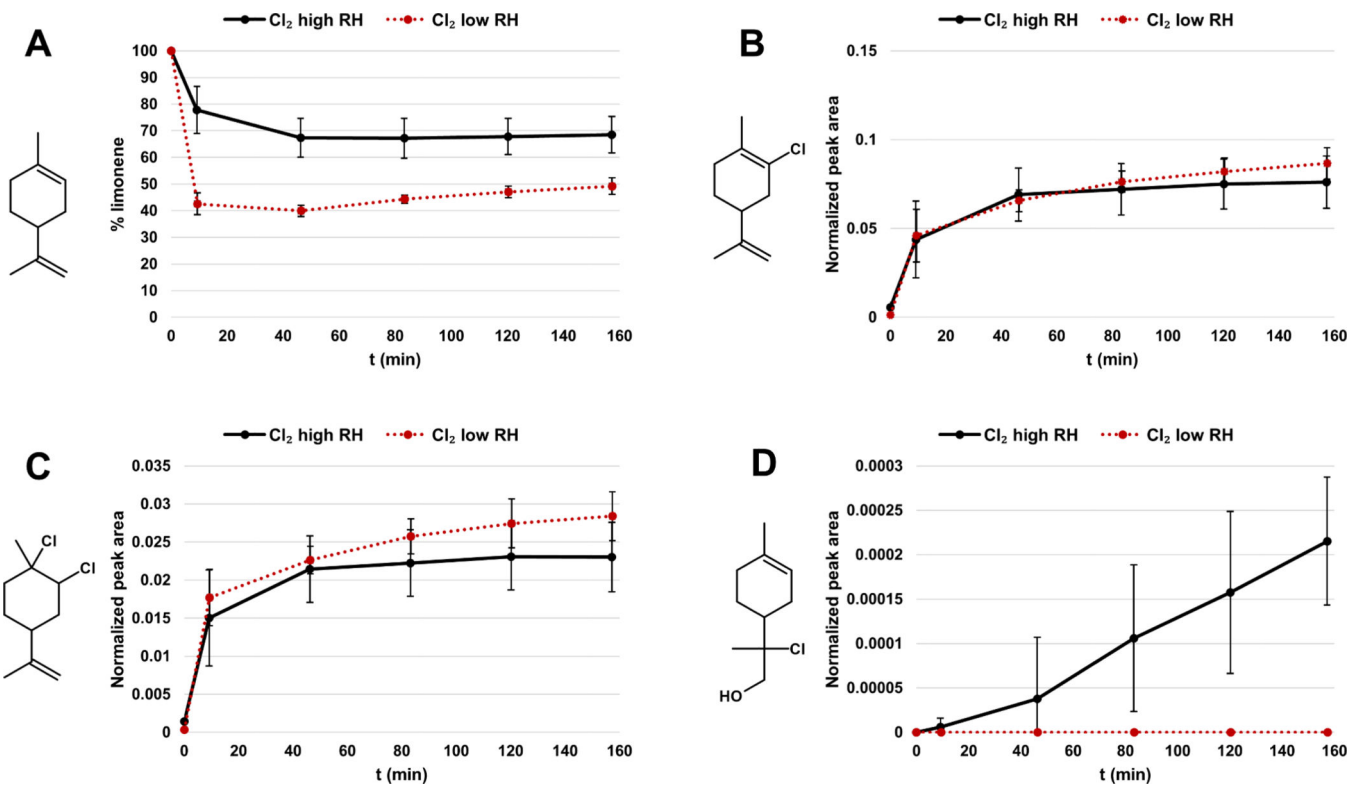
- (54). Chen J; Moller KH; Wennberg PO; Kjaergaard HG Unimolecular Reactions Following Indoor and Outdoor Limonene Ozonolysis. *J. Phys. Chem. A* 2021, 125 (2), 669–680. [PubMed: 33432816]
- (55). Kingston DGI; Hobrock BW; Bursey MM; Bursey JT Intramolecular hydrogen transfer in mass spectra. III. Rearrangements involving the loss of small neutral molecules. *Chem. Rev.* 1975, 75 (6), 693–730.
- (56). Lebedev AT; Detenchuk EA; Latkin TB; Bavcon Kralj M; Trebše P. Aqueous Chlorination of D-Limonene. *Molecules* 2022, 27 (9), 2988. [PubMed: 35566337]
- (57). Lim YB; Ziemann PJ Kinetics of the heterogeneous conversion of 1,4-hydroxycarbonyls to cyclic hemiacetals and dihydrofurans on organic aerosol particles. *Phys. Chem. Chem. Phys.* 2009, 11 (36), 8029–8039. [PubMed: 19727510]
- (58). United States Environmental Protection Agency. Estimation Programs Interface Suite for Microsoft Windows. EPI Suite-Estimation Program Interface, U.S. EPA (accessed February 2, 2024).
- (59). Nazaroff WW; Weschler CJ Indoor ozone: Concentrations and influencing factors. *Indoor Air* 2022, 32 (1), No. e12942.
- (60). Atkinson R; Hasegawa D; Aschmann SM Rate constants for the gas-phase reactions of O₃ with a series of monoterpenes and related compounds at 296 ± 2 K. *International Journal of Chemical Kinetics* 1990, 22 (8), 871–887.
- (61). NIOSH. NIOSH Pocket Guide to Chemical Hazards. Pocket Guide to Chemical Hazards, NIOSH|CDC (accessed January 9, 2024).
- (62). Goodson WH; Lowe L; Gilbertson M; Carpenter DO Testing the low dose mixtures hypothesis from the Halifax project. *Reviews on Environmental Health* 2020, 35 (4), 333–357. [PubMed: 32833669]
- (63). Rider CV; McHale CM; Webster TF; Lowe L; Goodson WH; La Merrill MA; Rice G; Zeise L; Zhang L; Smith MT Using the Key Characteristics of Carcinogens to Develop Research on Chemical Mixtures and Cancer. *Environ. Health Perspect.* 2021, 129 (3), No. 035003.

**Figure 1.**

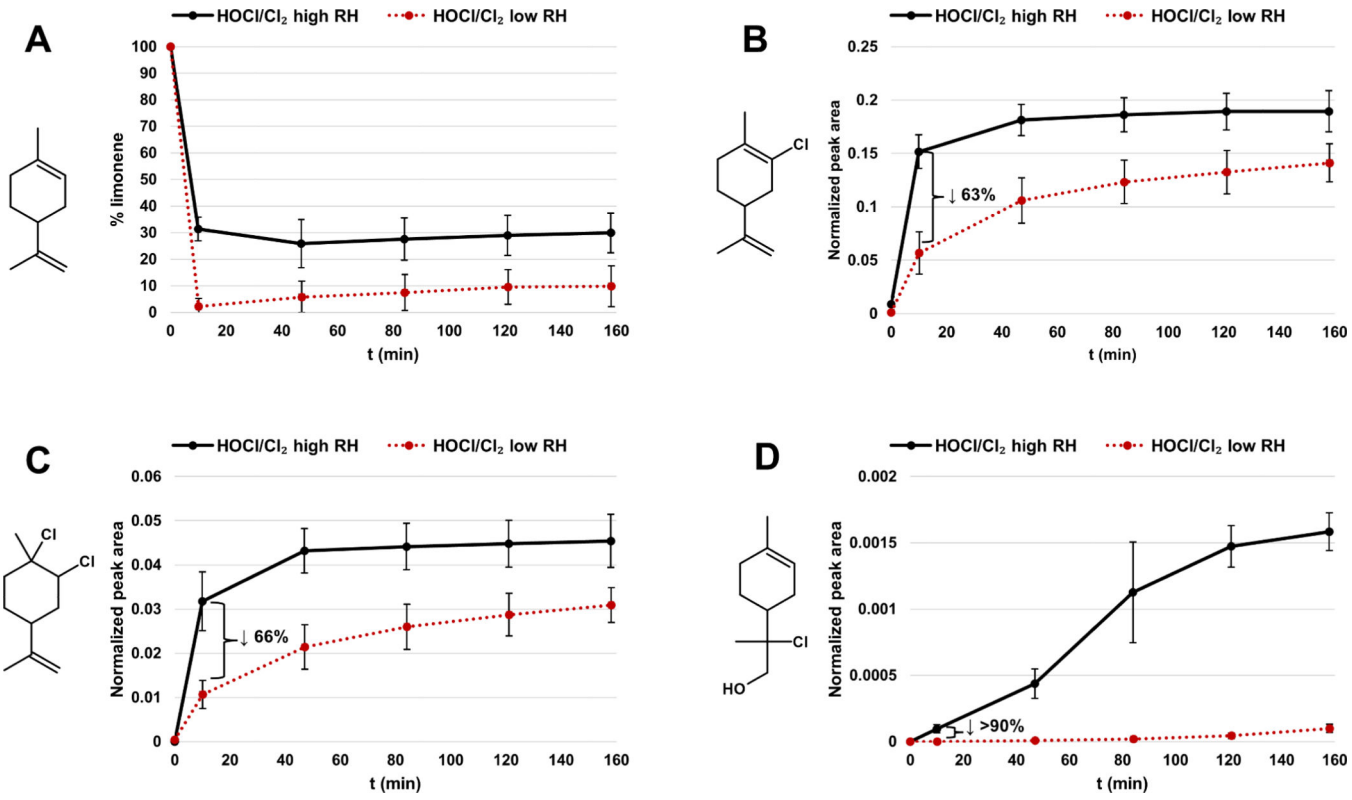
Effect of HOCl/Cl₂ on limonene and the generation of reaction products in gas-phase reactions. (A) Percentage of limonene remaining after exposure to HOCl/Cl₂ (black trace) and in the negative control treatment (red trace). Percentage pertains to the ratio between limonene concentration at each time point and concentration of limonene at time zero \times 100. Error bars indicate standard deviation with $n = 2$ for limonene and $n = 7$ for limonene + HOCl/Cl₂. (B) GC-MS TIC chromatogram comparison between gas phase chambers containing limonene (red trace) and limonene + HOCl/Cl₂ treatment (black trace). Limonene peak at RT 18.42 min is reduced to approximately 25% with HOCl/Cl₂ treatment. Numbers in red above the peak indicate species identified and are listed in Table 1.

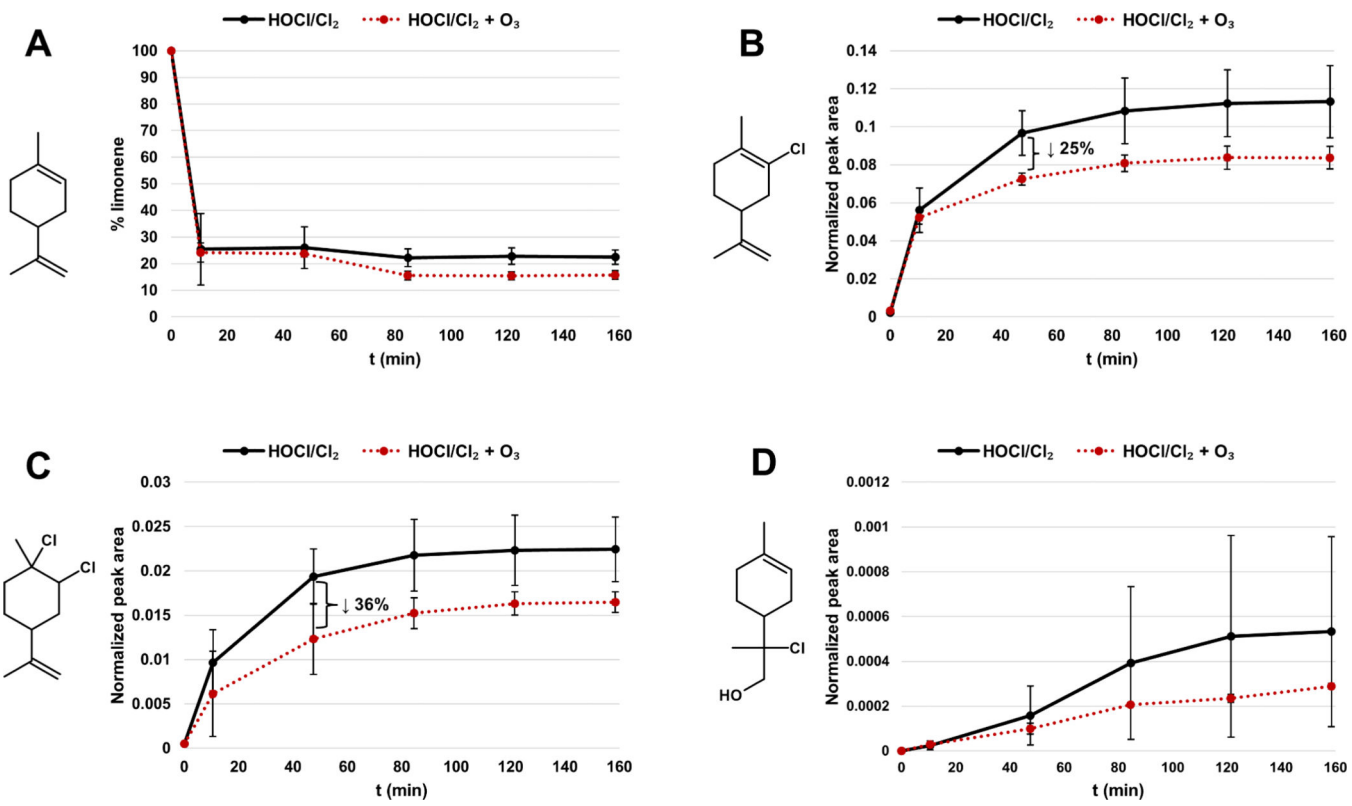
**Figure 2.**

Effect of Cl₂ (red dotted trace) and HOCl/Cl₂ (black trace) on limonene and its products in gas-phase reactions. (A) Comparison between effect of Cl₂ and HOCl/Cl₂ on decay of limonene. Percentage pertains to ratio between limonene concentration at each time point and concentration of limonene at time zero $\times 100$. (B) Comparison between effect of Cl₂ and HOCl/Cl₂ on singly chlorinated limonene (structure **1** in Table 1). (C) Comparison between effect of Cl₂ and HOCl/Cl₂ on dichlorinated limonene (structure **2**, Table 1). (D) Comparison between effect of Cl₂ and HOCl/Cl₂ on limonene chlorohydrin (structure **5**, Table 1). For B–D, the normalized peak area pertains to the peak area of each species divided by the peak area of limonene at time zero. Error bars represent standard deviation with $n = 3$ for limonene + HOCl/Cl₂ and $n = 7$ for limonene + Cl₂.

**Figure 3.**

Effect of 5% relative humidity (low, red dotted trace) and 50% relative humidity (high, black trace) on the reaction between limonene and Cl₂ in gas-phase reactions. (A) Comparison between the effect of low and high humidity on decay of limonene in the presence of Cl₂. Percentage pertains to ratio between limonene concentration at a given time point and concentration of limonene at time zero $\times 100$. (B) Comparison between the effect of low and high humidity on the formation of singly chlorinated limonene (structure 1, Table 1) in the presence of Cl₂. (C) Comparison between the effect of low and high humidity on the formation of dichlorinated limonene (structure 2, Table 1) in the presence of Cl₂. (D) Comparison between the effect of low and high humidity on the formation of limonene chlorohydrin (structure 5, Table 1). For B–D, the normalized peak area pertains to peak area of each species divided by peak area of limonene at time zero. Error bars represent standard deviation with $n = 7$ and 3 for high and low RH, respectively.



**Figure 5.**

Effect of ozone (30 ppb, red dotted trace) on the reaction between limonene and HOCl/Cl₂ in gas-phase reactions. Black trace pertains to addition of zero ppb of ozone. (A) The effect of ozone on decay of limonene in the presence of HOCl/Cl₂. Percentage pertains to ratio between limonene concentration at a given time point and concentration of limonene at time zero $\times 100$. (B) The effect of ozone on the formation of singly chlorinated limonene (structure **1**, Table 1) in the presence of HOCl/Cl₂. (C) The effect of ozone on the formation of dichlorinated limonene (structure **2**, Table 1) in the presence of HOCl/Cl₂. (D) The effect of ozone on the formation of limonene chlorohydrin (structure **5**, Table 1). For B–D, the normalized peak area pertains to peak area of each species divided by peak area of limonene at time zero. Error bars represent standard deviation with $n = 3$ and 4 for \pm ozone, respectively.

Chlorinated Products Detected in Gas-Phase Reactions between Limonene and HOCl/Cl₂

Compound	Limonene	1	2	3	4	5
Mol. Formula	C ₁₀ H ₁₆	C ₁₀ H ₁₅ Cl	C ₁₀ H ₁₆ Cl ₂	C ₁₀ H ₁₄ Cl ₂	C ₁₀ H ₁₅ Cl ₃	C ₁₀ H ₁₇ OCl
m/z	136.1247	170.0857	206.0624	204.0467	240.0234	188.0962
RT (min)	18.42	21.13 21.59 21.80	22.94 24.27	24.49 24.70	21.96 18.37	23.56 23.63